

See discussions, stats, and author profiles for this publication at: <https://www.researchgate.net/publication/7138214>

# Development of HPLC/ESI-MS and HPLC/H-1 NMR methods for the identification of photocatalytic degradation products of iodosulfuron

ARTICLE in ANALYTICAL CHEMISTRY · JUNE 2006

Impact Factor: 5.64 · DOI: 10.1021/ac051836t · Source: PubMed

---

CITATIONS

12

---

READS

34

6 AUTHORS, INCLUDING:



**Mohamad Sleiman**

Lawrence Berkeley National Laboratory

36 PUBLICATIONS 798 CITATIONS

SEE PROFILE



**Corinne Ferronato**

Claude Bernard University Lyon 1

78 PUBLICATIONS 1,627 CITATIONS

SEE PROFILE



**Bernard Fenet**

Claude Bernard University Lyon 1

126 PUBLICATIONS 1,367 CITATIONS

SEE PROFILE

# Development of HPLC/ESI-MS and HPLC/<sup>1</sup>H NMR Methods for the Identification of Photocatalytic Degradation Products of Iodosulfuron

Mohamad Sleiman,<sup>\*,†</sup> Corinne Ferronato,<sup>†</sup> Bernard Fenet,<sup>‡</sup> Robert Baudot,<sup>‡</sup> Farouk Jaber,<sup>§</sup> and Jean-Marc Chovelon<sup>†</sup>

Laboratoire d'Application de la Chimie à l'Environnement, UMR 5634, Université Claude Bernard Lyon 1, 43 Boulevard du 11 Novembre 1918, F-69622 Villeurbanne Cedex, France, Centre Commun de RMN UCB-CPE, F-69622 Villeurbanne Cedex, France, Service Central d'Analyse, USR 059 CNRS, Echangeur de Solaize, B.P. 22, 69390 Vernaison, France, and Laboratoire des Pesticides et des Micro-Polluants Organiques, Commission Libanaise de l'Energie Atomique, B.P. 11-8281, Riad El Solh, 1107 2260 Beirut, Lebanon

In the present study, HPLC/ESI-MS and stopped-flow HPLC/<sup>1</sup>H NMR methods were developed and applied to separate and characterize the byproducts arising from TiO<sub>2</sub>-catalyzed photodegradation of the herbicide iodosulfuron methyl ester (IOME) in aqueous solution under UV irradiation. Prior to identification, irradiated solutions of IOME (200 and 1000 mg·L<sup>-1</sup>) were concentrated by solid-phase extraction using two cartridges: Isolute C<sub>18</sub> and Isolute ENV<sup>+</sup>. Analytical separation was achieved on a C<sub>18</sub> reversed-phase column with ACN/H<sub>2</sub>O (HPLC/MS) or ACN/D<sub>2</sub>O (HPLC/NMR) as mobile phase and a linear gradient with a chromatographic run time of 35 min. The combination of UV and MS data allowed the structural elucidation of more than 20 degradation products, whereas <sup>1</sup>H NMR data permitted an unequivocal confirmation of the identities of major products and the differentiation of several positional isomers, in particular, the hydroxylation isomers. The obtained results permitted us to propose a possible degradation scheme and to put in evidence the presence of privileged sites for the attack of OH radicals. This work shows, for the first time, the application of combined HPLC with UV, MS, and NMR detection for complete structural elucidation of photocatalytic degradation products, and it will be of particular value in studies on the elimination of pollutants in aqueous solutions by photocatalysis.

In the past decades, heterogeneous photocatalysis has proved to be one of the most promising methods for the elimination of environmental pollutants.<sup>1–4</sup> This technique is based upon the use of UV-irradiated semiconductors, generally titanium dioxide

(TiO<sub>2</sub>), to produce strongly oxidizing species, usually hydroxyl radicals (OH•) which are able to destroy a great variety of toxic organic compounds. Ideally, the end products are carbon dioxide, water, and inorganic ions.

Generally, in this process, various byproducts are formed en route to complete mineralization. Some of them can be toxic, and in some cases, more persistent than the parent compound.<sup>5,6</sup> Therefore, a careful identification of these compounds is essential. Furthermore, this could be very useful to understand and interpret the degradation mechanism.

This task represents a particular analytical challenge because the majority of byproducts formed are new chemical entities, for which standards are not available. Moreover, several positional isomers are typically produced during the process. Thus, analytical methods that combine high separation efficiency with a maximum of structural information are required. GC/MS and LC/UV/MS techniques are the most frequently used.<sup>7–9</sup>

For byproducts of high to medium volatility which are thermally stable, GC/MS under electron impact (EI) conditions is the method of choice because it combines the high separation efficiency of the GC with the structural specificity of MS, and extensive MS libraries are available for the identification of already known analytes.

For polar thermally labile byproducts, such as those resulting from the photocatalytic degradation of sulfonylurea or phenylurea compounds, HPLC/UV-DAD and HPLC/MS are the techniques commonly used.<sup>10,11</sup> However, although these techniques are ideally suited to the characterization of known or suspected

\* Corresponding author. Tel: (33) 4 72 43 11 50. Fax: (33) 4 72 44 84 38. E-mail: mohamad.sleiman@univ-lyon1.fr.

<sup>†</sup> Université Claude Bernard Lyon 1.

<sup>‡</sup> Centre Commun de RMN UCB-CPE.

<sup>‡</sup> USR 059 CNRS.

<sup>§</sup> Commission Libanaise de l'Energie Atomique.

(1) Schiavello, M., Ed. *Photocatalysis and Environment: Trends and Applications*; NATO ASI Series C; Vol. 238; Kluwer Academic Publishers: London, 1987.  
(2) Ollis, D. F.; Al-Ekabi, H., Eds. *Photocatalytic Purification and Treatment of Water and Air*; Elsevier: Amsterdam, 1993.

(3) Blake, D. M. *Bibliography of Work on the Photocatalytic Removal of Hazardous Compounds from Water and Air*; NREL/TP-430-22197; National Renewable Energy Laboratory: Golden, CO, 1997 and 1999.  
(4) Herrmann, J. M. *Catal. Today* **1999**, *53*, 115–129.  
(5) Parra, S.; Sarria, V.; Malato, S.; Pèringer, P.; Pulgarin, C. *Appl. Catal., B* **2000**, *27*, 153–168.  
(6) Pramauro, E.; Bianco Prevot, A.; Vincenti, M.; Brizzolesi, G. *Environ. Sci. Technol.* **1997**, *37*, 3126–3131.  
(7) Koulombos, V. N.; Tsipi, D. F.; Hiskia, A. E.; Nikolic, D.; van Breemen, R. B. *J. Am. Soc. Mass Spectrom.* **2003**, *14*, 803–817.  
(8) Amorisco, A.; Losito, F.; Palmisano, F.; Zambonin, P. G. *Rapid Commun. Mass Spectrom.* **2005**, *19*, 1507–1516.  
(9) Calza, P.; Baudino, S.; Aigotti, R.; Baiocchi, C.; Pelizzetti, E. *J. Chromatogr., A* **2003**, *984*, 59–66.

byproducts, the structural elucidation of unknowns as well as the differentiation of the positional isomers remains difficult, even if MS/MS or MS<sup>n</sup> experiments is included.<sup>12</sup> As a result, the use of complementary techniques is necessary to get a full and unambiguous identification of byproducts.

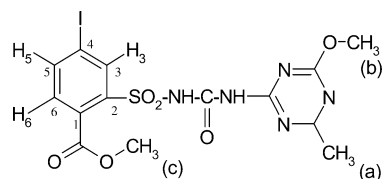
The HPLC/NMR technique is one of the most powerful methods for the structural elucidation of unknown compounds and the differentiation of structural isomers. It complements the HPLC/UV/MS methods well: whereas HPLC/MS provides important information on the molecular weight and the presence of certain functional groups, HPLC/NMR gives structural information on the constitution and the isomeric substitution of unknown molecules. Moreover, as a result of the very narrow resonance signals in modern high-field NMR, the resolution of information is also improved considerably and is comparable to that of GC/MS.<sup>13</sup>

The recent progress in pulse field gradients and solvent suppression, the improvements in probe technology, and the construction of high-field magnets have increased the sensitivity of the method and given a new stimulus to this technique, which has emerged since the mid 1990s as a very efficient tool for the on-line identification of organic molecules.

Nowadays, directly coupled HPLC/<sup>1</sup>H NMR spectroscopy is a commercially available technique that has been applied successfully in many cases in analytical chemistry, in particular to the identification of drug metabolites, natural products, and peptide libraries.<sup>14–20</sup> Furthermore, in the past few years, several studies have illustrated the capability of HPLC/NMR for the analysis of complex environmental samples, including the quantification of pollutants and their degradation products over an environmentally relevant range of concentrations.<sup>21–26</sup>

In this study, we present, for the first time, the application of combined HPLC/UV/MS and HPLC/<sup>1</sup>H NMR on-line coupling methods for an unequivocal identification of the byproducts resulting from the photocatalytic degradation of iodosulfuron (see

## Chart 1. Iodosulfuron Methyl Ester Chemical Structure



structure in Chart 1), a new member of the sulfonylurea group of herbicides which has recently entered our environment.

## EXPERIMENTAL SECTION

**Chemicals, Reagents, and Standards.** Iodosulfuron methyl ester (IOME) (methyl-4-iodo-2-[[[(4-methoxy-6-methyl-1,3,5-triazin-2-yl)-amino]carbonyl]amino]sulfonyl]-benzoate (>98%) was provided by Bayer Crop Science (Lyon, France). The following reference compounds for confirmation of the identified compounds were purchased from Aldrich (Steinheim, Germany): cyanuric acid [2,4,6-trihydroxy-1,3,5-triazine] (98%), ammeline [2-amino-4,6-dihydroxy-1,3,5-triazine] (97%) and s-triazine. For solubility and stability reasons,<sup>27</sup> stock solutions of IOME (200 and 1000 mg·L<sup>-1</sup>) were prepared in ultrapure water buffered with KH<sub>2</sub>PO<sub>4</sub>/K<sub>2</sub>HPO<sub>4</sub> at pH 6.5 and stored at 4 °C in the dark. The photocatalyst was TiO<sub>2</sub>, Degussa P-25, mainly anatase, with a specific area of 50 m<sup>2</sup> g<sup>-1</sup> and a mean particle size of 30 nm.

Acetonitrile (quality HPLC grade and quality NMR), methanol (HPLC grade), and deuterium oxide (99.9%) were purchased from SDS (Peypin, France). Water was obtained from a Millipore Waters Milli-Q water purification system (Molsheim, France). *ortho*-Phosphoric acid (85%) and formic acid (MS grade, 99% purity) were from Aldrich (Steinheim, Germany). Other reagents were of at least analytical grade.

**Irradiation Procedure.** The irradiation experiments were carried out in an open Pyrex glass cell (cutoff at 295 nm, 4.0-cm diameter, 2.3-cm height), containing 25 mL of the aqueous suspension of IOME and TiO<sub>2</sub> powder. The light source was a HPK 125 W Philips mercury lamp, cooled with water circulation. For all experiments, the cell temperature during irradiation was adjusted to 20 °C, the suspensions were magnetically stirred, and the concentration of TiO<sub>2</sub> was set to 2.5 g·L<sup>-1</sup>.

During the irradiation, aliquots of the aqueous suspension were collected at predefined times and filtered through 0.45-μm PVDF filters (Millipore) to remove TiO<sub>2</sub> particles.

**Solid-Phase Extraction (SPE).** To develop a sample extraction method adapted to a maximum number of degradation products which may have very different chemical properties and polarities (and a priori unknown), two types of SPE cartridges from International Sorbent Technology (IST, Cambridge, UK) were used: (a) Isolute C<sub>18</sub> (500 mg/6 mL), to extract IOME and its "first generation products" and (b) Isolute ENV<sup>+</sup> (200 mg/6 mL), a hydroxylated, highly cross-linked polystyrene/divinyl benzene copolymer (St-DVB) to concentrate more polar products as triazine derivatives.

The efficiency of the preconcentration of each of both used cartridges has been studied for different conditions (pH of the

- (10) Malato, S.; Caceres, J.; Fernandez-Alba, A. R.; Piedra, L.; Hernando, A. D.; Agüera, A.; Vial, J. *Environ. Sci. Technol.* **2003**, *37*, 2516–2524.
- (11) Vulliet, E.; Emmelin, C.; Chovelon, J. M.; Guillard, C.; Herrmann, J. M. *Appl. Catal., B* **2002**, *38*, 127–137.
- (12) Rafqah, S.; Wong-Wah-Chung, P.; Aamili, A.; Sarakha, M. J. *Mol. Catal. A: Chem.* **2005**, *237*, 50–59.
- (13) Preiss, A.; Levsen, K.; Humpfer, E.; Spraul, M. *Fresenius' J. Anal. Chem.* **1996**, *356*, 445–451.
- (14) Albert, K. J. *Chromatogr., A* **1999**, *856*, 199–211.
- (15) Lindon, J. C.; Nicholson, J. K.; Wilson, I. D. *J. Chromatogr., B* **2000**, *748*, 233–258.
- (16) Sandvoss, M.; Weltring, A.; Preiss, A.; Levsen, K.; Wuensch, G. *J. Chromatogr., A* **2001**, *917*, 75–86.
- (17) Peng, S. X. *Biomed. Chromatogr.* **2000**, *14*, 430–441.
- (18) Bobzin, S. C.; Yang, S. T.; Kasten, T. P. *J. Chromatogr., B* **2000**, *748*, 259–267.
- (19) Wolfender, J. L.; Ndjoko, K.; Hostettmann, K. *Phytochem. Anal.* **2001**, *12*, 2–22.
- (20) Wilson, I. D.; Lindon, J. C.; Nicholson, J. K. *Anal. Chem.* **2000**, *72*, 534–542.
- (21) Levsen, K.; Preiss, A.; Godejohann, M. *Trends Anal. Chem.* **2000**, *19*, 27–48.
- (22) Benfenati, E.; Pierucci, P.; Fanelli, R.; Preiss, A.; Godejohann, M.; Astratov, M.; Levsen, K.; Barceló, D. J. *Chromatogr., A* **1999**, *831*, 243–256.
- (23) Preiss, A.; Sängler, U.; Karfich, N.; Levsen, K.; Mügge, C. *Anal. Chem.* **2000**, *72*, 992–998.
- (24) Godejohann, M.; Preiss, A.; Mügge, C.; Wünsch, G. *Anal. Chem.* **1997**, *69*, 3832–3837.
- (25) Godejohann, M.; Astratov, M.; Preiss, A.; Levsen, K.; Mügge, C. *Anal. Chem.* **1998**, *70*, 4104–4110.
- (26) Godejohann, M.; Preiss, A.; Mügge, C. *Anal. Chem.* **1998**, *70*, 590–595.

- (27) Brigante, M.; Emmelin, C.; Previtera, L.; Baudot, R.; Chovelon, J. M. *J. Agric. Food Chem.* **2005**, *53*, 5347–5352.

sample; nature, composition, and volume of eluting solution). The best extraction conditions were conditioning of the sorbents with 6 mL of MeOH followed by 6 mL of pure water. The sorbents were not allowed to dry, and subsequently irradiated samples of IOME (200 and 1000 mg·L<sup>-1</sup>) of 20 mL volume were passed through the cartridges at a rate of ~3 mL·min<sup>-1</sup> using a Varian vacuum manifold (Sigma-Aldrich). For the ENV<sup>+</sup> cartridge, the pH of the samples was adjusted to between 2.5 and 2.7 using 40% orthophosphoric acid. The analytes were eluted using 1 mL of MeOH (2 × 0.5 mL) at a rate of ~1 mL·min<sup>-1</sup>.

**HPLC Separations.** Optimization of HPLC separations were carried out on a 150 × 3 mm i.d., Interchim HDO C<sub>18</sub> (Montluçon, France) reversed-phase column (3 μm, 128 Å) using a Shimadzu VP series HPLC system (Kyoto, Japan) consisting of a LC-10AT binary pump, a SPD-M10A DAD, and Shimadzu Class-VP software (version 5.0). The mobile phase was a mixture of acetonitrile (A) and water acidified with formic acid to pH 2.8 (B). The flow rate was set to 0.4 mL·min<sup>-1</sup>, and injection volumes were 20 μL. The optimized linear gradient was programmed as follows: 0 min, 5% A; 30 min, 70% A; 33 min, 70% A; and 35 min, 100% A.

**HPLC/MS Experiments.** The HPLC/MS analysis was performed on a HP 1100 (Agilent Technologies, Waldbronn, Germany) LC system (Hewlett-Packard GmbH) consisting of quaternary pump, degasser, autosampler, column oven, and DAD UV detector, interfaced with a HP 1100 MSD quadrupole mass spectrometer equipped with an electrospray ionization source. The chromatographic conditions were similar to those of the HPLC separations (see HPLC Separations).

In preliminary experiments, an optimization of the ESI interface and ion optics parameters was accomplished to maximize the ionization current signal of the analytes. For this purpose, a 200 mg·L<sup>-1</sup> IOME irradiated solution was infused (flow rate 20 μL·min<sup>-1</sup>) into the ESI interface using the syringe pump incorporated into the mass spectrometer.

The optimized electrospray parameters were spray voltage, 4 kV; cone voltage, 80 V; drying gas (nitrogen), 12 L·min<sup>-1</sup>; nebulizer pressure, 55 psi; and source temperature, 350 °C. Mass spectra were detected in both positive and negative ion modes in a mass range of *m/z* 80–1000.

**HPLC/NMR Stopped-Flow Experiments.** Experiments were conducted on an Agilent 1100 series HPLC system consisting of a solvent degasser (model G1322A), a quaternary pump, a manual injector (model 7725i) from Rheodyne (Rohnert Park, U.S.A.) and a VWD (variable wavelength detector). A BSFU (Bruker stop flow unit) was used to interface the HPLC to a DRX 500-MHz NMR spectrometer from Bruker (Rheinstetten, Germany). The NMR spectrometer was equipped with a <sup>1</sup>H–{<sup>13</sup>C} inverse flow probe (3-mm i.d. of measuring cell, with a detection volume of 60 μL). The chromatographic equipment was controlled by HyStar NT version 2.3 software (Bruker, Germany). Stopped-flow NMR spectra were acquired using XWINNMR software (version 3.5, Bruker, Rheinstetten, Germany).

The chromatographic separation was performed using ACN and (D<sub>2</sub>O + H<sub>3</sub>PO<sub>4</sub>, pH 2.8) as mobile phase. D<sub>2</sub>O was used for the deuterium lock to ensure stable measurement conditions. In addition, formic acid used in the HPLC/MS experiments was replaced by *ortho*-phosphoric acid to avoid superposition of the signals of the analytes and formic acid in the aromatic spectral

region. The analytical column and gradient were the same as used for the HPLC/MS experiments.

Prior to data acquisition, solvent-signal suppression was achieved using water suppression enhanced through T<sub>1</sub> effects (WET) solvent suppression, which included standard 4-fold selective excitation with 20-ms seduced-1 pulses flanked by 1-ms sine-shaped gradient pulses, with GARP <sup>13</sup>C decoupling during WET dephasing and acquisition to suppress <sup>13</sup>C satellites of ACN.<sup>28</sup> FIDs were collected into 16-K data points (spectral width of 10 000 Hz) with a flip angle of 90° and a relaxation delay of 3.0 s, resulting in a total repetition time of 4.1 s. Depending on the concentration of the analyte in the sample, the total number of scans varied between 64 and 256. After acquisition, data were multiplied with an exponential function *f2* leading to a line broadening of 0.3 Hz (LB = 0.3 Hz) prior to Fourier transformation. <sup>1</sup>H NMR chemical shift values were referenced to acetonitrile, which was set to 2.0 ppm.

**Safety Considerations.** Iodosulfuron, ammelide and *s*-triazine are toxic compounds and should, therefore, be handled with special care. UV light used for irradiation is harmful to the eyes, and a UV mask must be used for protection.

## RESULTS AND DISCUSSION

**SPE Preconcentration.** After optimization of the conditions, experiments were performed in triplicate. Recoveries were determined by comparing the analytes' UV responses before and after preconcentration, taking into account the preconcentration factor, which is theoretically equal to 20.

Using the C<sub>18</sub> cartridge, good recoveries (58–83%, RSD < 9%) were obtained for IOME and its degradation products **11–21** (see Table 1), whereas for the highly polar products (**1–10**), such as triazine derivatives, the preconcentration efficiency was unsatisfactory, with poor recoveries ranging from 8 to 21% (RSD < 13%). As a consequence, the C<sub>18</sub> cartridge was not suitable for the preconcentration of the polar products.

Using the ENV<sup>+</sup> cartridge, extraction efficiency was much better for the highly polar products (**1–10**), with satisfactory recoveries between 38 and 54% (RSD < 8%) except for cyanuric acid, which had a moderate recovery of 32 ± 5%. For the less polar products, such **11–21**, ENV<sup>+</sup> allowed us to obtain acceptable recoveries, but lower than with the C<sub>18</sub> (42–61%, RSD < 11%).

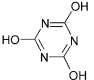
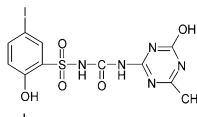
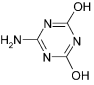
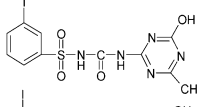
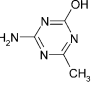
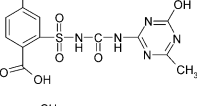
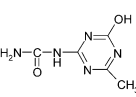
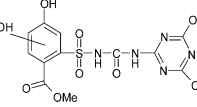
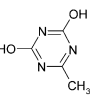
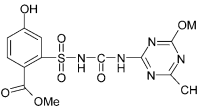
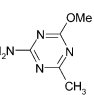
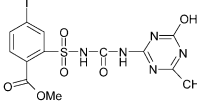
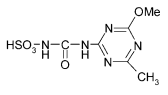
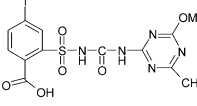
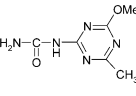
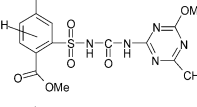
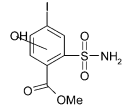
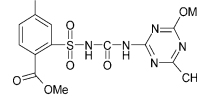
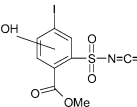
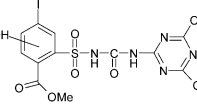
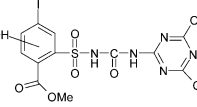
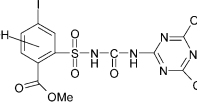
Study of recoveries obtained with the two tested cartridges (C<sub>18</sub> and ENV<sup>+</sup>) shows well that the use of both cartridges was appropriate to make an efficient preconcentration of the degradation products of IOME to detect and identify them further by HPLC/MS and HPLC/NMR.

**HPLC/UV/ESI-MS.** The characterization of byproducts was first achieved by HPLC/UV/ESI-MS. As described in the Experimental Section, the MS spectra were acquired in both positive and negative ion modes to confirm the structural assignment of the quasimolecular ion, [M + H]<sup>+</sup> in positive ion mode by the corresponding molecular anion [M – H]<sup>–</sup>. By comparing the two ionization modes, the first was found to be more sensitive and suitable for the majority of the analyzed compounds. Thus, all the detected byproducts form [M + H]<sup>+</sup> ions, but only some of these, that is, **4**, **6–8**, and **14–21**, form [M – H]<sup>–</sup> ions, as well

(28) Smallcombe, S. H.; Patt, S. L.; Keifer, P. A. *J. Magn. Reson. A* **1995**, *117*, 295–303.



**Table 1. UV and MS Data for the Structural Characterization of IOME and Its Photocatalytic Transformation Products**

Product	Structure	$R_t^a$ (min)	UV data ( $\lambda_{max}$ , nm)	MS data ESI, pos./neg mode	Product	Structure	$R_t^a$ (min)	UV data ( $\lambda_{max}$ , nm)	MS data ESI, pos./neg mode
1		2.0	198, 224	152 (M+Na) <sup>+</sup> 130 (M+H) <sup>+</sup>	11		15.6	232, 286	473(M+Na) <sup>+</sup> 451(M+H) <sup>+</sup> 153, 127
2		2.4	200, 226	151(M+Na) <sup>+</sup> 129 (M+H) <sup>+</sup>	12		17.0	230, 282	457(M+Na) <sup>+</sup> 435(M+H) <sup>+</sup> 153, 127
3		3.0	195, 225	127 (M+H) <sup>+</sup>	13		18.0	235, 290	502(M+Na) <sup>+</sup> 480(M+H) <sup>+</sup> 153, 127
4		3.6	198, 230	192 (M+Na) <sup>+</sup> 170(M+H) <sup>+</sup> 127, 153 168(M-H) <sup>-</sup>	14		18.7	230, 284	436 (M+Na) <sup>+</sup> 414(M+H) <sup>+</sup> 167, 141 412 (M-H) <sup>-</sup>
5		4.8	197, 230	150 (M+Na) <sup>+</sup> 128 (M+H) <sup>+</sup>	15		19.4		
6		6.4	196, 226,	141 (M+H) <sup>+</sup> 139 (M-H) <sup>-</sup>	16		20.1	231, 293	420 (M+Na) <sup>+</sup> 398 (M+H) <sup>+</sup> 167 396 (M-H) <sup>-</sup>
7		7.7	198, 229	264 (M+H) <sup>+</sup> 184 (M-SO <sub>3</sub> ) <sup>+</sup> 167, 141 262 (M-H) <sup>-</sup>	17		20.8	232, 295	516 (M+Na) <sup>+</sup> 494 (M+H) <sup>+</sup> 127 492 (M-H) <sup>-</sup>
8		10.0	199, 226	206(M+Na) <sup>+</sup> 184(M+H) <sup>+</sup> 167, 141 182 (M-H) <sup>-</sup>	18		21.3	234, 297	516 (M+Na) <sup>+</sup> 494 (M+H) <sup>+</sup> 167, 141 492 (M-H) <sup>-</sup>
9		11.1	246, 288	328 (M+Na) <sup>+</sup> 306 (M+H) <sup>+</sup>	19		23.8	234, 298	546 (M+Na) <sup>+</sup> 524 (M+H) <sup>+</sup> 167, 141 522 (M-H) <sup>-</sup>
10		12.7	240, 290	404(M+Na) <sup>+</sup> 382 ((M+H) <sup>+</sup>	IOME		27.7	234, 288	524 (M+Na) <sup>+</sup> 508 (M+H) <sup>+</sup> 167, 141 506 (M-H) <sup>-</sup>
					20		28.1		
					21		28.7	234, 298	546 (M+Na) <sup>+</sup> 524 (M+H) <sup>+</sup> 167, 141 522 (M-H) <sup>-</sup>

<sup>a</sup>  $R_t$ : Retention time.

(see Table 1). This could be explained by the presence of nitrogen atom(s), having an important proton affinity (basic character), in the majority of the byproducts.

Figure 1 depicts the UV trace recorded at 234 nm and ESI-MS full-scan (positive mode) chromatograms, obtained for a mixture of three aqueous solutions of IOME (200 mg·L<sup>-1</sup>) irradiated successively for 15 min, 1 h, and 3 h. On the basis of a preliminary monitoring by HPLC/DAD of the degradation products during 5 h of irradiation, this mixture represents as much as possible the different byproducts formed during the degradation. As can be seen in Figure 1, many compounds in addition to IOME are present in the analyzed sample. The majority of these

products are eluted before IOME, which is normal because the photocatalytic process involves the formation of smaller and more polar products when compared to the parent compound; however, some compounds are eluted after IOME, and thus, they are more hydrophobic than IOME. Mass spectra of some of these products showed very high masses ( $m/z > 600$ ), indicating that they probably result from reactions of dimerization. This hypothesis was supported by the absence of these compounds when the degradation experiment was achieved at low levels of concentrations of IOME (<100 mg·L<sup>-1</sup>). Structures of these later-eluted compounds were not determined and will not be discussed here. In contrast, structures of the majority of compounds eluted before

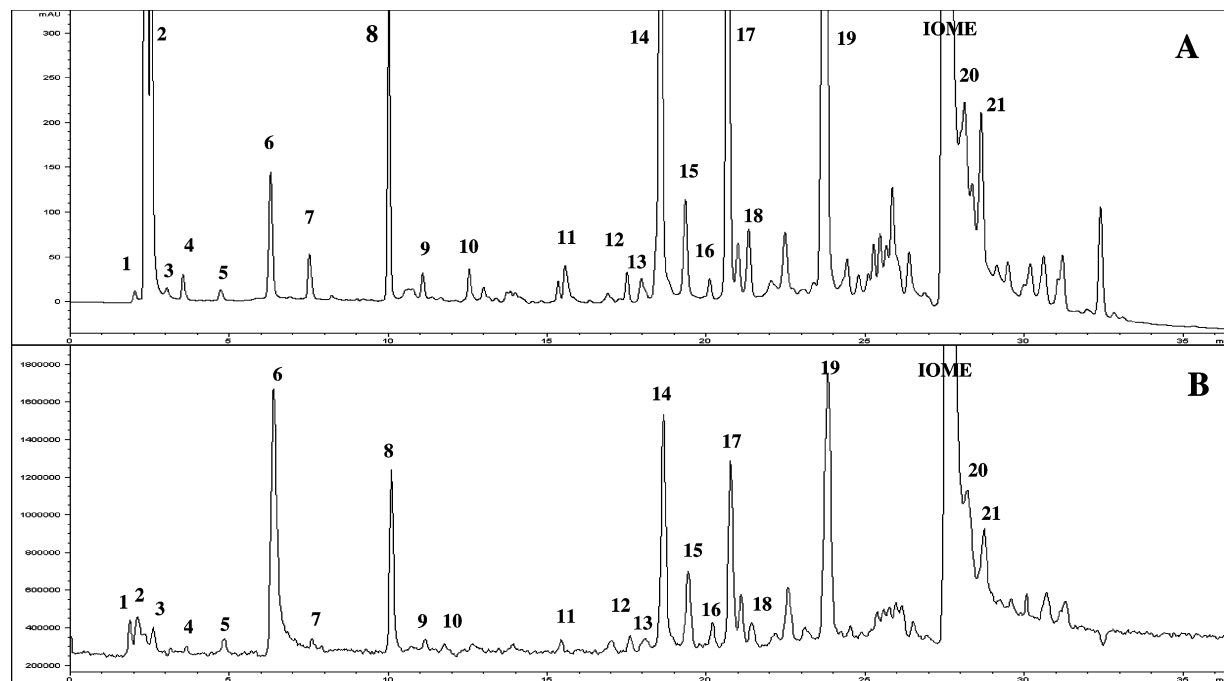


**Figure 1.** HPLC/UV at 234 nm (A) and HPLC/ESI-MS in positive mode (B) chromatograms of a mixture of three aqueous solutions of IOME ( $200 \text{ mg} \cdot \text{L}^{-1}$ ) irradiated successively for 15 min, 1 h, and 3 h. For chromatographic conditions, refer to the Experimental Section. Peak numbers correspond to compound numbers in Table 1.

30 min (Figure 1) were tentatively identified by interpretation of their UV and MS spectra. A summary of the UV and MS data (absorption maximums, quasimolecular ions, and the most important fragment ions), along with the proposed structures for the byproducts, is reported in Table 1.

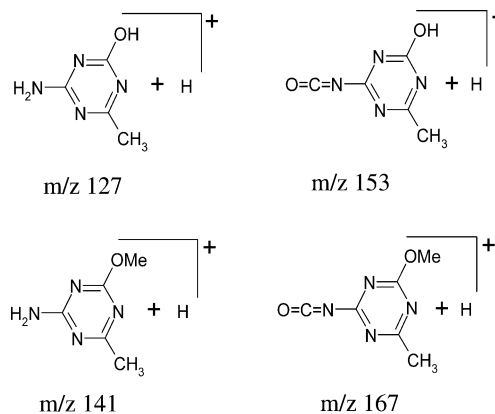
The identified byproducts can be classified in three principal groups according to their structures:

(a) *Byproducts 1–8.* These early-eluting, highly polar compounds showed UV spectra (not shown) typical of a triazine ring with two maximums between 195 and 200 and 220–230 nm (Table 1). No absorption band was observed above 270 nm, suggesting the absence of a benzene ring in their structures. This conclusion was corroborated by the mass spectrometric data which revealed quasimolecular ( $127\text{--}264$ ) and fragment ions ( $127, 153, 141, 167$ ) compatible with structures of triazine derivatives (see Table 1).

The identities of byproducts **1**, **2**, and **6** were confirmed by direct comparison of their UV, MS, and chromatographic data with those of reference compounds cyanuric acid, ammeline, and *s*-triazine (AMMT), respectively. These compounds were previously reported in several studies on the photocatalytic degradation of sulfonyleureas.<sup>11,29</sup>

The remaining byproducts were not commercially available, and therefore, a confirmation of their identities was relatively difficult. However, byproducts **4**, **7**, and **8** exhibit some characteristic fragment ions in positive ion ESI-MS, providing further structural information. Thus, the MS spectrum of byproduct **4** showed two main fragment ions at  $m/z$  127 and 153. The first is interpreted as arising from cleavage of the bond between the carbonyl group and the N-atom substituted with the triazinic group, whereas the second is due to the cleavage of the carbonyl C–NH<sub>2</sub> bond. By analogy, formation of fragment ions at  $m/z$  141

**Chart 2. Chemical Structures of the Main Fragment Ions,  $m/z$  127, 141, 153 and 167, Observed in MS Spectra of IOME Byproducts**



and 167 in MS spectra of byproducts **7** and **8** can be rationalized. The structures of the identified fragments ( $m/z$  127, 141, 153, 167) are shown in Chart 2. It should be pointed out that this type of fragmentation was already observed for sulfonyleurea products by Marek and Koskinen.<sup>30</sup>

(b) *Byproducts 9, 10.* UV spectra of these two products were typical of a benzene ring with two bands between 240 and 250 (band I) and between 285 and 290 nm (band II). This, along with the  $[M + H]^+$  quasimolecular ions and  $[M + Na]^+$  adducts detected in their MS spectra suggests that these two byproducts correspond to the structures proposed in Table 1. Unfortunately, the MS data did not provide more detailed structural information to determine the position of hydroxyl group on the benzene ring, so that several isomers can be hypothesized for these compounds.

(29) Maurino, V.; Minero, C.; Pelizzetti, E.; Vincenti, M. *Colloids Surf., A* **1999**, *151*, 329–338.

(30) Marek, L.; Koskinen, W. J. *Agric. Food Chem.* **1996**, *44*, 3878–3881.

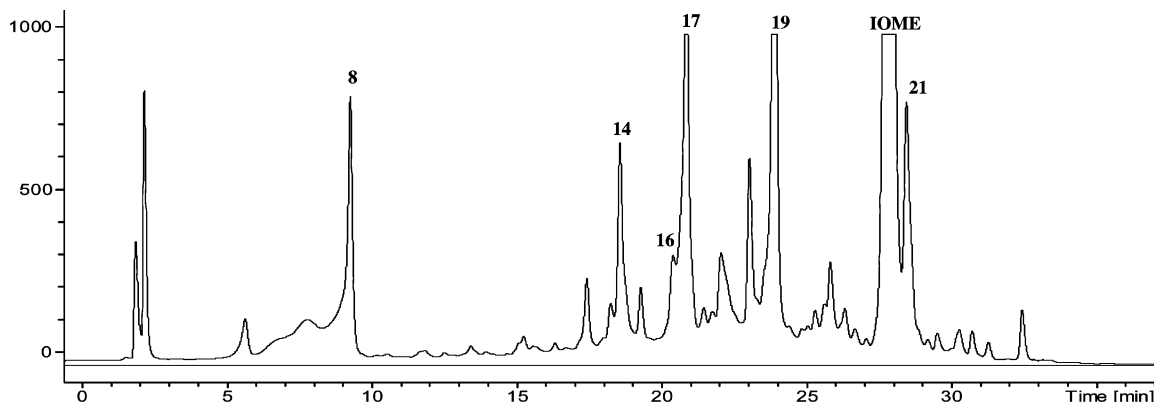


**Figure 2.** HPLC/UV chromatogram (234 nm) as obtained from the Stopped-flow LC/NMR run of a concentrated solution of IOME 1000 mg·L<sup>-1</sup>.

(c) *Byproducts 11–21.* These products were characterized by high retention times (> 15 min, Figure 1), indicating that they are less polar than those of the first two groups (a, b), their structures are likely to contain the two moieties (benzene and triazine rings). This was verified by comparing the UV spectra of these compounds with that of IOME with two characteristic bands between 225 and 235 nm (band I) and 280–300 nm (band II), indicating the presence of the two rings. Furthermore, MS spectra of these products revealed, as already observed for byproducts of group (a), characteristic fragment ions at  $m/z$  127, 153 (byproducts **11–13**, **17**) or at  $m/z$  141, 167 (**14–16**, **18–21**) which proves that they contain the triazine ring. On the other hand, these fragment ions permitted knowing whether a byproduct contains a triazinic ring substituted with OH and CH<sub>3</sub> groups ( $m/z$  127 and 153) or with OCH<sub>3</sub> and CH<sub>3</sub> ( $m/z$  141 and 167). As a consequence, we have distinguished the two isomers **17** and **18** having the same mass ( $[M + H]^+$  at  $m/z$  494) considering that compound **17** gave the two fragment ions at  $m/z$  127 and 153, whereas the MS spectrum of byproduct **18** showed the two other fragment ions at  $m/z$  141 and 167.

In contrast, the information provided by mass spectrometry was not sufficient to make the differentiation between the positional isomers **14**, **15** (two isomers) and **19–21** (three isomers), resulting from the attack of OH· on the benzene ring. Therefore, HPLC/<sup>1</sup>H NMR coupling was used to determine the substitution pattern of the aromatic ring for these isomers and also to verify the structure assignment by HPLC/UV/MS of those compounds for which reference compounds were not available, in particular, the group of byproducts **11–21**.

**Stopped-Flow HPLC/<sup>1</sup>H NMR.** Since the sensitivity of the NMR detection is low compared to MS, more concentrated samples of IOME (1000 mg·L<sup>-1</sup>) were irradiated and, later on, preconcentrated by SPE (as described in Experimental Section). Moreover, volumes of 100 μL were injected instead of 20 μL.

The UV chromatogram at 234 nm as obtained in the stop-flow mode for a mixture of three solutions of IOME (1000 mg·L<sup>-1</sup>) irradiated for 45, 150, and 480 min is depicted in Figure 2. These irradiation times permitted us to obtain a mixture that contains the different byproducts at their maximum levels of concentrations. Noting that the degradation of IOME (1000 mg·L<sup>-1</sup>) was completely achieved within ~160 min, as compared to 60 min for the solution of IOME at 200 mg·L<sup>-1</sup>, which is normal because the degradation of higher concentrations need more UV irradiation time.

By comparing the chromatogram displayed in Figure 2 with that showed in Figure 1, it can be seen that the use of D<sub>2</sub>O as the mobile phase and the replacement of formic acid by phosphoric acid had no significant effect on the elution order and the retention times of the main byproducts. Therefore, a correlation between the HPLC/MS peaks in Figure 1 and the HPLC/NMR peaks in Figure 3 was exploited to identify as many IOME byproducts as possible. As a result, the structures of six major byproducts, **8**, **14** (isomer of **15**), **16**, **17** (isomer of **18**), **19** and **21** (two monohydroxylation isomers), were unambiguously identified. Figure 3 shows relevant regions of the corresponding <sup>1</sup>H NMR spectra and that of IOME, obtained in the stopped-flow mode. The <sup>1</sup>H NMR signal assignments are summarized in Table 2.

According to Figure 3, spectrum A corresponding to the parent compound (IOME) is divided in two sections, an aliphatic region (2–4 ppm) displaying the protons of the methyl groups (a–c) and an aromatic region (7–8.5 ppm) showing the signals of a 1,2,4 trisubstituted aromatic system: a doublet with a small meta coupling constant for H<sub>3</sub>, a doublet of doublet with a small meta and a large ortho coupling constant for H<sub>5</sub>, and a doublet with a large ortho coupling constant for H<sub>6</sub>. Signals of NH protons are missing because of their exchange with deuterium in the D<sub>2</sub>O matrix. Note that the signal at 3.3 ppm corresponds to methanol, which is the solvent in which the injected samples were dissolved after preconcentration.

In comparison, it can be noted that aliphatic regions of <sup>1</sup>H NMR spectra B, C, and D are almost identical to that of IOME, revealing the presence of a methyl group around 2.5 ppm (a), a methyl ester group around 3.9 ppm (c), and a methoxy group around 4.0 ppm (b). On the other hand, the aromatic parts of spectra B–D show only two signals integrated for 1 H each, indicating the substitution of one of the three aromatic protons by a hydroxyl group (OH). This finding is supported by the chemical shift values of the aromatic protons and by the MS data.

Byproduct **21** (spectrum C) exhibits two ortho-coupling doublets centered at 8.17 and 6.95 ppm ( $J \sim 8.0$  Hz), which are assigned to H<sub>5</sub> and H<sub>6</sub>, respectively. Thus, the proton H<sub>3</sub> was substituted by a hydroxyl group (OH). In contrast, the aromatic pattern of byproducts **14** (isomer of **15**) and **19** (isomer of **21**) reveal two singlets (see spectra B and D) corresponding to the noncoupled protons H<sub>3</sub> and H<sub>6</sub>. The OH group is thereby located in position 5 (C<sub>5</sub>) on the aromatic ring (Table 2).

Unfortunately, byproducts **15** (isomer of **14**) and **20** (isomer of **19** and **21**) were not identified because of their low concentra-

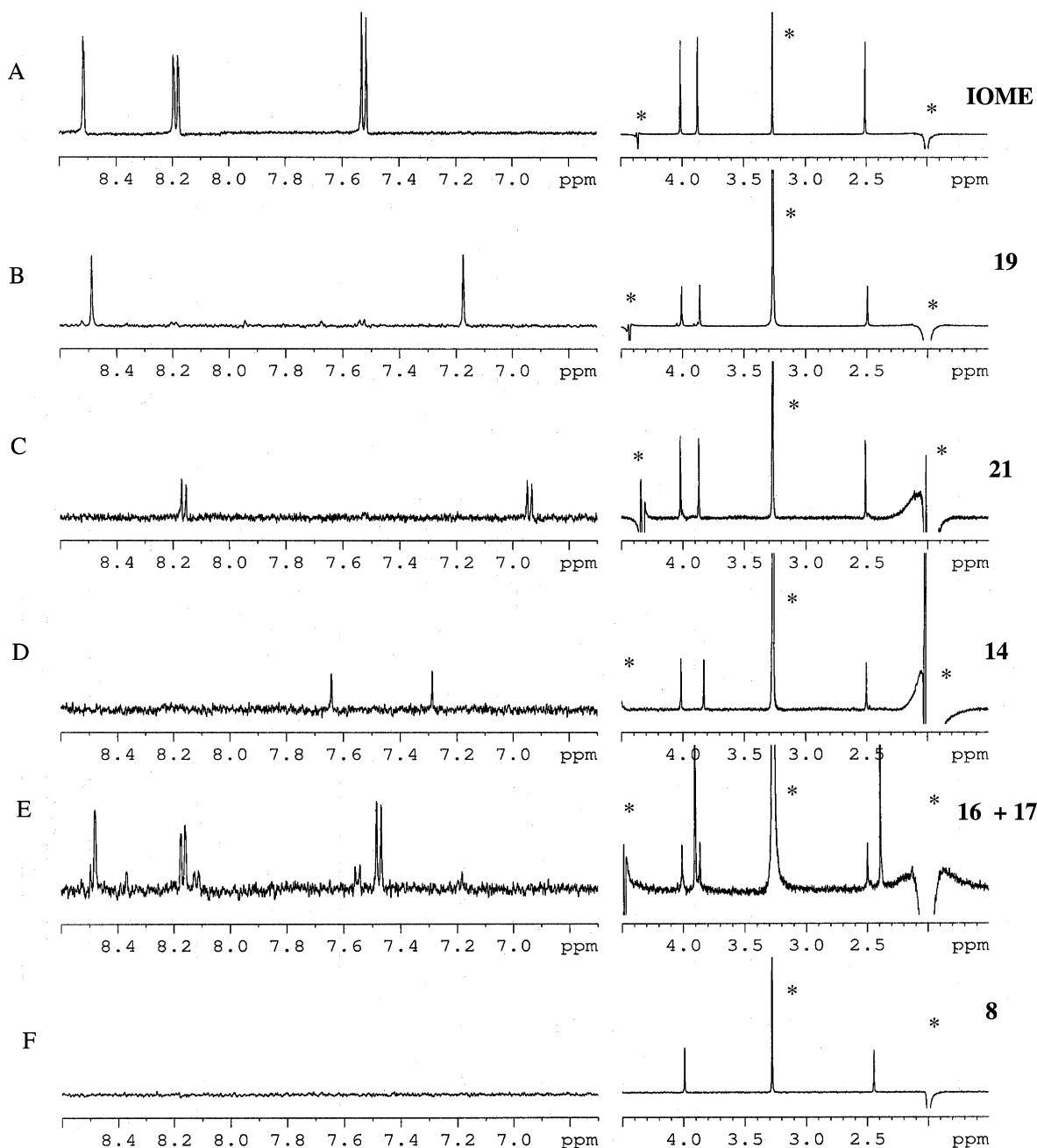


**Figure 3.** Stopped-flow  $^1\text{H}$  NMR spectra of IOME (A) and its byproducts **19** (B), **21** (C), **14** (D), **16** and **17** (E), and **8** (F). An asterisk (\*) denotes residual solvent signals (ACN, 1.93 ppm; MeOH, 3.30 ppm; HOD  $\sim$  4.5 ppm).

tions and their overlapping with other chromatographic peaks. Nevertheless, the structure of isomer **20** could be assigned taking into account that only one free site (position 6) remains for the OH function to be on the aromatic ring, since the two others, positions 5 and 3, were already attributed to isomers **19** and **21**, respectively.

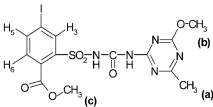
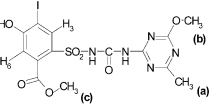
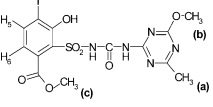
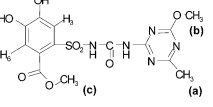
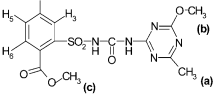
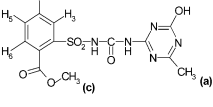
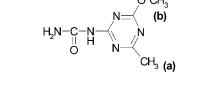
A closer look at spectrum E, extracted at  $\sim$ 21 min, shows two groups of signals probably resulting from a mixture of two byproducts. Indeed, the chromatographic peak at  $\sim$ 21 min (see Figure 3) exhibits a left threshold which indicates a coelution process. Comparison with the separation profile in the HPLC/UV/MS experiments (Figure 1) suggests that the two coeluted byproducts are likely to be **16** (minor) and **17** (major). This suggestion and the structures of both byproducts were confirmed

by the interpretation of the  $^1\text{H}$  NMR signals of spectrum E: in the aliphatic region, the two intense singlets are attributed to the methyl group (a) and the methyl ester group (c) of byproduct **17**, whereas the three remaining singlets of weak intensities correspond to the methyl group (a), the methyl ester group (c), and the methoxy group (b) of byproduct **16** (Table 2). On the other hand, in the aromatic region, each product exhibits three signals (two doublets of doublets and one doublet) assigned to the aromatic protons  $\text{H}_3$  (d),  $\text{H}_5$  (dd), and  $\text{H}_6$  (dd) (see Table 2).

Finally, contrary to the preceding spectra A–E, spectrum F does not show any signals in the aromatic part, indicating the absence of a benzene ring. The aliphatic region displays only two singlets, which might be assigned to the methyl group (a) and the methoxy group (b). This information is not sufficient to deduce



**Table 2.  $^1\text{H}$  NMR Data for IOME and Its Byproducts Identified by Stopped-Flow HPLC/NMR**

Product	Structure	$R_t$ (min)	NMR data ( $\delta$ -values, multiplicities <sup>(a)</sup> , coupling constants)
IOME		27.6	$H_3$ : 8.52 (d, $J_{3,5}$ 1.7 Hz), $H_5$ : 8.19 (dd, $J_{5,6}$ 8.1 Hz, $J_{3,5}$ 1.7 Hz), $H_6$ : 7.52 (d, $J_{5,6}$ 8.1 Hz), $H_a$ : 2.50 (s), $H_b$ : 4.02 (s), $H_c$ : 3.87 (s)
19		23.8	$H_3$ : 8.48 (s), $H_6$ : 7.18 (s), $H_a$ : 2.50 (s), $H_b$ : 4.02 (s), $H_c$ : 3.86 (s)
21		28.5	$H_5$ : 8.17 (d, $J_{5,6}$ 8.0 Hz), $H_6$ : 6.95 (d, $J_{5,6}$ 8.0 Hz), $H_a$ : 2.50 (s), $H_b$ : 4.02 (s), $H_c$ : 3.86 (s)
14		18.7	$H_3$ : 7.64 (s), $H_6$ : 7.29 (s), $H_a$ : 2.50 (s), $H_b$ : 4.01 (s), $H_c$ : 3.83 (s)
16		20.2	$H_3$ : 8.37 (d, $J_{3,5}$ 1.5 Hz), $H_5$ : 8.13 (dd, $J_{3,5}$ 1.5 Hz, $J_{5,6}$ 8.3 Hz), $H_6$ : 7.56 (d, $J_{5,6}$ 8.3 Hz), $H_a$ : 2.50 (s), $H_b$ : 4.02 (s), $H_c$ : 3.87 (s)
17		20.8	$H_3$ : 8.49 (d, $J_{3,5}$ 1.6 Hz), $H_5$ : 8.17 (dd, $J_{3,5}$ 1.7 Hz, $J_{5,6}$ 8.2 Hz), $H_6$ : 7.49 (d, $J_{5,6}$ 8.1 Hz), $H_a$ : 2.40 (s), $H_c$ : 3.90 (s)
8		9.2	$H_a$ : 2.46 (s), $H_b$ : 4.0 (s)

<sup>a</sup>  $R_t$ : Retention time. <sup>b</sup> s, singlet; d, doublet; dd, doublet of doublet.

the complete structure of the compound because each one of byproducts **6**, **7**, and **8** has both methyl groups a and b and can thereby give almost the same  $^1\text{H}$  NMR spectrum. However, due to the fact that the peaks' retention times in both chromatograms (Figures 1 and 2) are almost identical, spectrum F, which is extracted at  $\sim 10$  min corresponds well to byproduct **8** having a  $[\text{M} + \text{H}]^+$  at  $m/z$  184 in the MS spectrum.

**Deductions Concerning the Photocatalytic Degradation of IOME.** On the basis of the foregoing results of the LC/UV/MS and LC/NMR experiments, a general reaction pathway can be proposed for the photocatalytic degradation of IOME (Scheme 1). Although this task would be difficult starting only from the identification of the intermediates, some considerations about the process can be made:

(i) The first steps of the degradation seem to be hydroxylation of the benzene ring, O-demethylation of the methoxy and methyl ester moieties, substitution of the iodide atom by a hydroxyl group, and cleavages of the sulfonyleurea bridge. This means that the products **3**, **4**, and **6–21** might be formed during the initial degradation of IOME (see Scheme 1).

(ii) The hydroxylation process leads to three isomeric products, **19**, **20**, and **21**. By assuming that the response coefficients for the three isomers in UV or MS detection (Figure 1) are relatively similar, it is clear that **19** is the major reaction product. This

indicates that  $\text{C}_5$  on the benzene ring of IOME is privileged for the attack of OH radicals. This result might be explained by the mesomeric effect of the benzene ring substituents ( $-\text{COOMe}$ ,  $-\text{SO}_2$ , and  $-\text{I}$ ). The groups  $-\text{COOMe}$  and  $-\text{SO}_2$  decrease the electron density in ortho and para positions ( $\text{C}_3$ ,  $\text{C}_5$ , and  $\text{C}_6$ ) with respect to them, whereas the iodide atom increases the electron density in ortho and para positions ( $\text{C}_3$  and  $\text{C}_5$ ) with respect to it. Therefore, sites  $\text{C}_3$  and  $\text{C}_5$  are more nucleophilic than site  $\text{C}_6$ , which explains the formation of byproducts **19** and **21** at higher levels of concentration than that of byproduct **20** (not identified). On the other hand, attack of OH radicals on position 3 is more difficult than that on position 5 because of the steric hindering by the  $-\text{SO}_2$  group. As consequence, the attack of OH radicals, known as strong electrophilic species, takes place preferentially at  $\text{C}_5$  and forms compounds **19**.

(iii) The substitution of an iodide atom by hydroxyl groups forms the byproduct **16**, which in turn can be transformed by a hydroxylation process into the two products **14** and **15**. These compounds could be also formed by substitution of an iodide atom of the hydroxylation products **19–21** by a hydroxyl group.

(iv) Byproducts **17** and **18** result from an O-demethylation of the methoxy moiety of the triazine ring and the methyl ester groups, respectively. Both products can undergo a second O-demethylation, leading to byproduct **13**. Decarboxylation via

## Scheme 1. Proposition of Photocatalytic Degradation Pathway of IOME

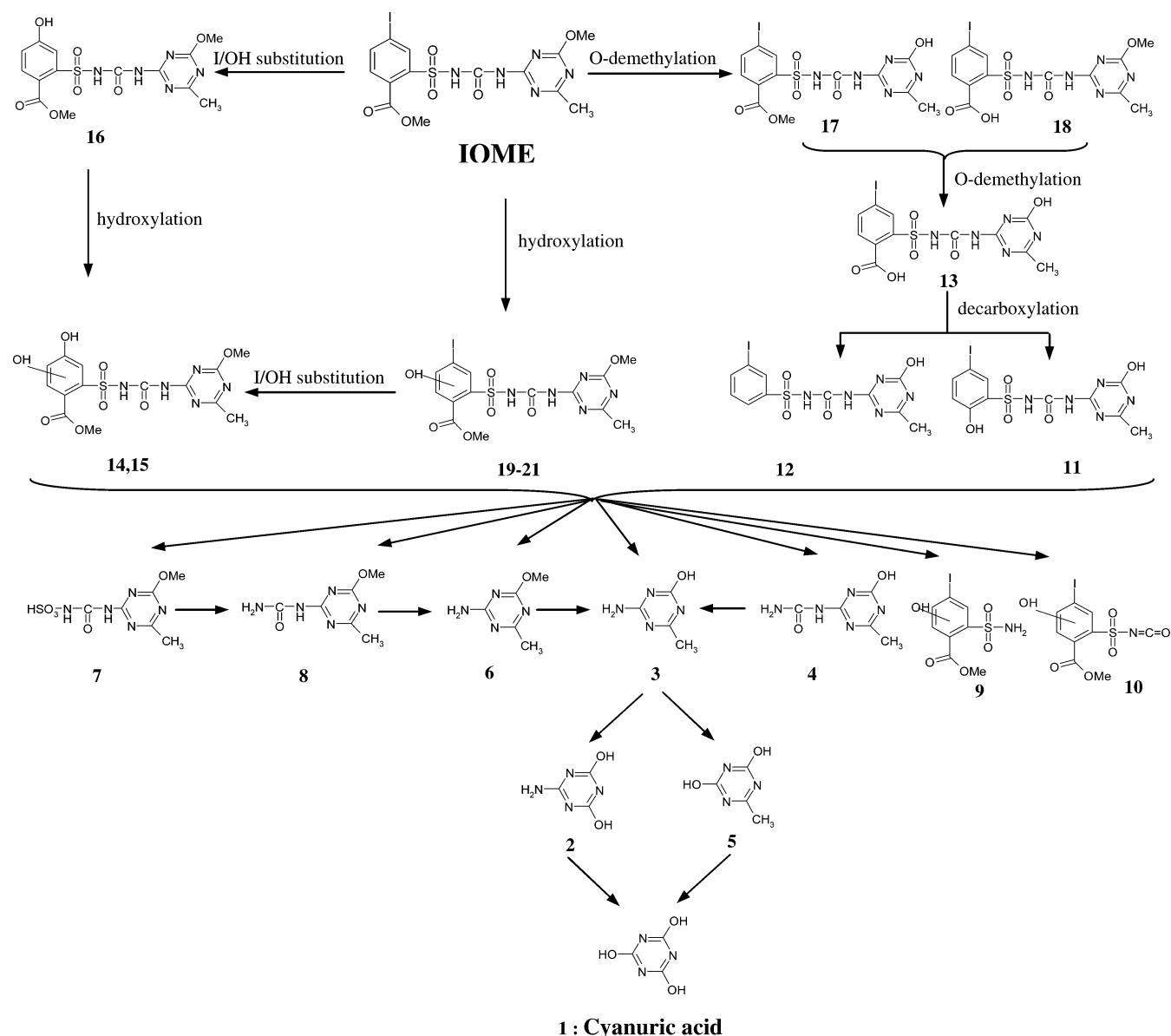


photo-Kolbe reactions<sup>31</sup> can be invoked to justify the formation of compounds **11** and **12** from **13**.

(iv) Cleavages of the sulfonylurea bridge of IOME and its products **11**–**21** generate various *s*-triazinic derivatives (**3**, **4**, **6**–**8**) dominated by the products **6** and **8** resulting from the rupture of carbon–nitrogen (C–N) and nitrogen–sulfur (N–S) bonds, respectively. Cleavage of the sulfonylurea bridge also leads to the formation of benzene derivatives. Only two of them were detected and identified during the degradation process (byproducts **9** and **10**). This could be attributed to the fact that they are rapidly transformed by an oxidative opening of the aromatic ring, giving rise to the formation of smaller and more oxidized molecules, such as short carboxylic acids (formic, acetic, oxalic, etc). This behavior has been confirmed in a previous study in which several carboxylic acids, such as formic, acetic, oxalic and glycolic acids, have been detected after the aromatic ring opening.<sup>11,32</sup>

(v) The formation of other *s*-triazinic compounds, such as products **2** and **5**, suggests that the degradation process continues via a series of reactions, including further cleavages of the sulfonylurea bridge, O-demethylation of the methoxy moiety of the triazine, and oxidation of methyl and amino groups leading to cyanuric acid (**1**), which cannot undergo further oxidative attacks. It constitutes a final product, as has been observed in previous studies.<sup>11,28,33</sup>

## CONCLUSIONS

The combined use of HPLC/UV/MS and HPLC/NMR under similar chromatographic conditions was demonstrated to be a very powerful approach for the identification of a large number of compounds generated by photocatalytic transformation of IOME, even if no reference compounds are

(31) Krautler, B.; Bard, A. J. *J. Am. Chem. Soc.* **1978**, *10*, 2239.

(32) Pramauro, E.; Vincenti, M.; Augugliaro, V.; Palmisano, L. *Environ. Sci. Technol.* **1993**, *27*, 1790–1795.

(33) Pelizzetti, E.; Maurino, V.; Minero, C.; Carlin, V.; Pramauro, E.; Zerbini, O.; Tosato, M. L. *Environ. Sci. Technol.* **1990**, *24*, 1559–1565.

commercially available. This approach could be further applied successfully for the structural elucidation of byproducts resulting from the treatment of others pollutants by photocatalysis.

On the basis of the results of the identification of byproducts, a general scheme of degradation in which cyanuric acid was the final organic product has been proposed. Fortunately, this compound is known to be innocuous, nontoxic, and easily biodegradable; thus, its formation during the photocatalytic process does not represent any danger to the environment and human beings.

Taking into account the results obtained during this study, it would be interesting to quantify the main byproducts identified using HPLC/NMR, since at a given concentration, the signal intensity depends only on the molecular mass and the number of chemical equivalent protons. In addition, an evaluation of the toxicity of the different byproducts would be essential for the continuation of this study.

Received for review October 13, 2005. Accepted March 6, 2006.

AC051836T